Molecular Crystals and Liquid Crystals Science and Technology. Section A. Molecular Crystals and Liquid Crystals

Publication details, including instructions for authors and subscription information:
http://www.tandfonline.com/loi/gmcl19

Polymer Dispersed Liquid Crystals Based on Epoxy Networks: Transformations and Phase Separation Phenomena During Polycondensation

H. Masood Siddiqi [a], M. Dumon [a] & J. P. Pascault [a]

[a] Laboratoire des Matériaux Macromoléculaires-CNRS UMR n°5627, Institut National des Sciences Appliquées de Lyon, 20, Avenue A. Einstein, F-69621, Villeurbanne, cedex, France

Version of record first published: 04 Oct 2006

To cite this article: H. Masood Siddiqi, M. Dumon & J. P. Pascault (1998): Polymer Dispersed Liquid Crystals Based on Epoxy Networks: Transformations and Phase Separation Phenomena During Polycondensation, Molecular Crystals and Liquid Crystals Science and Technology. Section A. Molecular Crystals and Liquid Crystals, 312:1, 137-155

To link to this article: http://dx.doi.org/10.1080/10587259808042437

Mol. Cryst. Liq. Cryst., 1998, Vol. 312, pp. 137–155
Reprints available directly from the publisher
Photocopying permitted by license only

Polymer Dispersed Liquid Crystals Based on Epoxy Networks: Transformations and Phase Separation Phenomena During Polycondensation

H. MASOOD SIDDIQI, M. DUMON* and J. P. PASCAULT

Laboratoire des Matériaux Macromoléculaires – CNRS UMR n°5627, Institut National des Sciences Appliquées de Lyon; 20, Avenue A. Einstein F-69621 Villeurbanne cedex, France

(Received 27 May 1997; In final form 18 September 1997)

A diepoxy-diamine / liquid crystal mixture (50/50 wt%) is studied in the course of the crosslinking step-polymerization at different isothermal reaction temperatures or with a two temperature cure cycle. Depending on the reaction temperature, the systems undergoe phase separation either isothermally, when the reaction temperature is far below the nematic-isotropic (N-I) temperature of the neat LC, or on cooling partially reacted systems when the reaction temperature is above the N-I temperature of the neat LC.

Phase separation is characterized simultaneously by two glass transition temperatures (T_g), one nematic-isotropic transition ($T_{N\text{-}I}$) and the appearance of nematic droplets as determined by differential scanning calorimetry (DSC) or polarized optical microscopy (POM). Thus, temperature-polymerization conversion phase diagrams are presented in the form of the evolution of T_g's and of $T_{N\text{-}I}$ of the LC-rich phase. Furthermore, we attempted to use the calorimetric data to calculate the mass fraction of the LC-rich phase and the mass fraction of separated LC.

The gel point conversions of the epoxy-amine network are determined. For example, $T_{N\text{-}I}$ of the LC phase markedly increases near the gel point during an isothermal crosslinking at 30°C.

The observation of the PDLC samples confined between two glass plates showed that final morphology (at full conversion) depends strongly on the thermal cycles of crosslinking.

Finally, for a cure at 100°C, in bulk samples, evidence is given for a macrosyneresis of the LC in the fully crosslinked network. However, this phenomenon occurs very slowly with time. This means that depending on the cure cycles, on the LC content and on the confinement of the LC, the resulting PDLC may be prepared in off equilibrium conditions.

Keywords: Polymer dispersed liquid crystals; phase separation; polymerization; Temperature – conversion phase diagrams; gelation; morphology

* Corresponding author.

INTRODUCTION

Polymer dispersed liquid crystals (PDLC) are composite materials formed by dispersions of liquid crystal droplets in a polymer matrix [1]. The embedded mesophase results in an electrosensitive film, e.g. that can be switched from a light scattering state to a transparent state. The functional properties, mostly electro-optical, of these composite materials are very dependent on their morphology which is a result of a demixing process. PDLC are obtained by the phase separation of the liquid crystal (LC) from a homogeneous LC/polymer, or LC/monomer(s) or oligomer(s) solutions [2]. Depending upon the type of the polymer used, phase separation can be induced either by thermal quench (TIPS), by solvent evaporation (SIPS) or by polymerization (PIPS). The latter technique is mostly used when the polymer matrix is a network. A summary of this technique related to modified thermosetting structural polymers may be found in reference [3].

More specifically, epoxy resins with hardeners have been used in previous studies [4–12] to provide network matrices for PDLC applications. These contributions highlight some major factors that affect the morphology, i.e. the size, shape and the densiy of the LC droplets. These factors are either thermodynamical (solubility of LC in the polymer phase, initial phase diagram, type of material used), or chemical (rate of polycondensation) or rheological (viscosity of polymer) or else the rate of diffusion of the LC.

Because the separated phase can be an anisotropic phase (e.g. nematic), a question arising about phase separation is the nature of driving force responsible for the initial demixing during polymerization i.e., whether a liquid–liquid separation due to the increase in molar mass of the epoxy-amine copolymer or a liquid-ordered phase (nematic) separation due to the tendency of the LC molecules to organize themselves. This question has been little investigated both theoretically and experimentally. W. Ahn *et al.* [13] have concluded that a polymer/LC blend presents a liquid–liquid equilibrium when the critical temperature (T_C) is higher than $T_{I\text{-}N}$ of the neat LC. In their experiment, they mention the difficulty of detecting a liq.–liq. phase separation when the refractive indices of both phases are close to each other. Kato *et al.* [14] have also shown that, if $T_{I\text{-}N} > T_C$, they find an isotropic-nematic phase separation and for $T_{I\text{-}N} < T_C$ they have an isotropic-isotropic phase separation. T. Kyu *et al.*, have provided a thermodynamic expression for the free energy of mixing based on the Flory Huggins theory and the Maier Saupe expression [15–18]. In the case of crosslinked polymers, the description of the free energy of mixing needs an additional term depending upon the concentration of elastically active

network chains [19–20]. This term is responsible for the phenomenon of "syneresis" in network/solvent systems.

In a previous paper [21], we studied the effects of a nematic LC addition on the epoxy-amine reaction: rate constants, different reactivities of primary and secondary amino groups, but also the different structural transformations during the epoxy-amine network formation. This study was performed as a function of the epoxy conversion for three LC compositions, 10, 30, 50% bw. We have reported that out of the three systems cured at 100°C, only the 50% bw showed phase separation after cooling at room temperature. In the present paper, we study this 50/50% bw LC/epoxy-amine system. The epoxy-amine reaction is carried out at two reaction temperatures T_i = 30 or 100°C chosen according to their proximity to the nematic-isotropic (N-I) transition of the neat LC. The aim of the present work is to study the phase separation and the morphology in the course of polymerization.

EXPERIMENTAL

Materials

The monomers used are the diglycidyl ether of bisphenol A, DGEBA (DER 332 $\bar{n} = 0.03$, DOW) with a hardener namely polypropylene oxide diamine, Jeffamine (D-400, $\bar{x} = 5.6$, HUNTSMAN). The LC used is a mixture of cyano bi and terphenyls (E7 from Merck). The description of these compounds and the synthetic path are given in a previous paper [21].

Techniques

Two techniques were used to study the phase separation: differential scanning calorimetry (DSC) and polarized optical microscopy (POM). The monitoring of the reaction kinetics and the phase separation kinetics were performed simultaneously by DSC and POM.

A Mettler TA 3000 calorimeter was used to measure, at different stages of the epoxy-amine reaction, the residual polymerization enthalpy and the resulting epoxy conversion $x = 1 - (\Delta H/\Delta H_0)$ [21] but also the glass transition temperatures, T_g, the change in heat capacity, ΔC_p at T_g, the nematic to isotropic transitions, $T_{N\text{-}I}$, and the enthalpy of nematic to isotropic transitions, $\Delta H_{N\text{-}I}$. The glass transition was considered as the temperature mid point between the tangents of the two base lines above and below the transition region. $T_{N\text{-}I}$ was taken as the maximum of the

endothermic peak of the N-I transition. The rate of heat flow was chosen at 10 K/min under argon atmosphere. Scans were recorded between −100°C and 320°C. The DSC samples were prepared as follows: several DSC pans, containing the reactive 50/50% bw LC/epoxy-amine mixture, were cured isothermally at 30°C or 100°C to different times or conversions. For each conversion, the reaction was stopped by cooling down the sample in liquid nitrogen and the pan was immediately scanned by DSC between −100°C and 320°C.

At the same time, samples between glass plates were cured at the same reaction temperature and were observed under POM. The POM is a Leica Laborlux 12 POLS provided with a hot stage Mettler FP 82 and a camera. The POM samples were prepared as follows: glass plates are filled by capillary action, the thickness of the samples was estimated to be smaller than 10 microns. Then they were kept at the reaction temperature and after different intervals of time, temperature was decreased to room temperature from 100°C at a controlled rate, without any previous quenching in liquid nitrogen, or were observed isothermally at 30°C for samples cured at 30°C. The temperature at which a birefringent texture begins to appear was taken as the isotropic to nematic transition temperature ($T_{I\text{-}N}$). The temperature at which the birefringent texture completely vanishes on heating was taken as the nematic to isotropic transition temperature ($T_{I\text{-}N}$). The cooling rate is 1 K/min.

A home-made image processing software was used to determine the average diameter of LC particles from micrographs. More than 100 particles were analyzed to obtain an average diameter.

Small Angle X-Ray Scattering experiment was performed to follow the phase separation at a complementary observation scale. A lab set-up was used which composed of a rotating anode X-ray generator with copper target and nickel filter ($\lambda = 1.54$ Å), a point collimation produced mainly by two orthogonal mirrors and a line position sensitive proportional counter connected to a computer. The sample was heated *in-situ* from room temperature to the selected polymerization temperature, T_i. A 10 minute counting time provided a good signal to noise ratio.

RESULTS AND DISCUSSION

Reactive Blends Cured Isothermally at One Temperature, T_i

We will first consider the systems cured at 30°C, a temperature lower than $T_{N\text{-}I}$ of the neat liquid crystal (61°C) and then the systems cured at 100°C, a temperature much higher than the $T_{N\text{-}I}$ of the neat liquid crystal.

At T_i = 30°C, phase separation occurs during cure in the form of birefringent points (small particles) which can be detected when their size is around 1 μm. The cloud point conversion for which the droplets can be detected under polarized microscope at 30°C isothermally (without any clooing) is $x_{cp} \approx 0.45$. The conversion at gelation of this system is $x_{gel} = 0.48$ [21]. The birefringent particles grow with conversion isothermally at 30°C from $x = 0.45$ up to $x = 0.85$. The isothermal evolution of the average droplets diameter is given in Figure 1. The observation of the particle growth is consistent with a nucleation-growth mechanism where the driving force for phase separation is the increase in average molar mass.

The evolution with conversion of the different transition temperatures, as measured by DSC on a heating ramp but after a cooling from 30°C to −100°C, is represented in Figure 2. In the early stages, conversion $x < 0.35$, the thermograms show only one glass transition temperature in the range of −54°C to −50°C. This T_g is attributed to that of a homogeneous mixture of the epoxy-amine *i*-mers and the liquid crystal. T_{gLC} of the neat LC being −63°C and the T_{gEA} of the monomers being −51°C, applying the Fox equation [23], we get a T_g value for the initial mixture T_{g_o} = −57°C. This value is in good agreement with the measured one of −54°C.

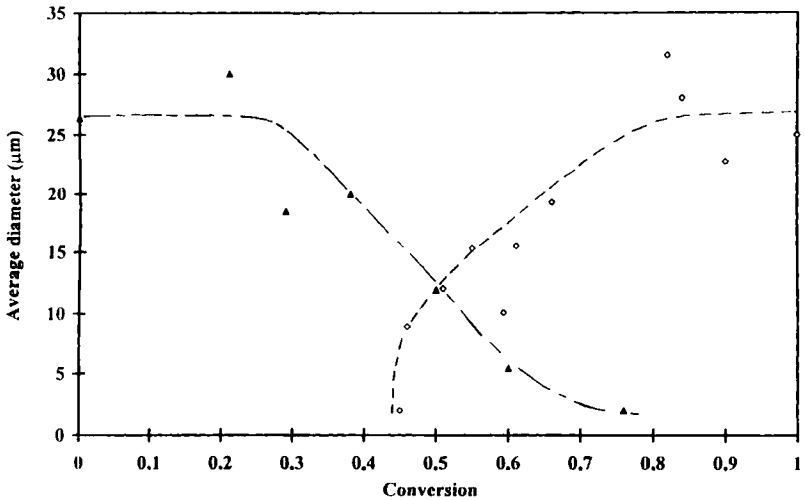

FIGURE 1 Average diameter of LC droplets as a function of epoxy conversion in different reaction conditions.

▲ PDLC cured at T_i = 100°C till x_{100} and then post cured at 30°C up to full conversion.
The diameter is that at full conversion ($x_{100} + x_{30} = 1$).
The conversion plotted is that attained at 100°C (x_{100}).

◇ PDLC cured isothermally at 30°C.
The diameter and the conversion plotted are those attained at 30°C (x_{30}).

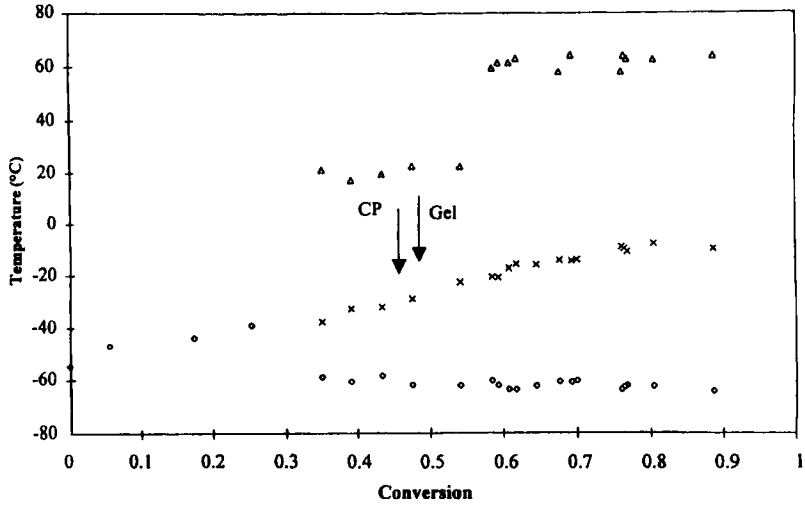

FIGURE 2 Conversion dependence of the different transition temperatures for the 50% b/w LC system cured at 30°C and then scanned between −100°C and 320°C at a rate of 10 K/min. ▲ $T_{N\text{-}I}$ × $T_{g\alpha}$ ◇ $T_{g\beta}$.

Then, for $x > 0.35$, the thermograms exhibit two glass transitions and an endothermic peak ($\Delta H_{N\text{-}I}$ and $T_{N\text{-}I}$). The lower glass transition temperature ($T_{g\beta}$) and the endothermic peak are attributed to a LC-rich phase (β-phase) whereas the higher glass transition temperature ($T_{g\alpha}$) corresponds to a polymer-rich phase (α-phase). The fact that a two phase structure is obtained for $x = 0.35$ indicates that the LC is not totally soluble in the epoxy-amine *i*-mers with such an advancement of reaction. At $x = 0.35$, phase separation results from both an increase in average molar mass of the epoxy-amine copolymer and from the cooling process (30°C to −100°C) of the DSC measurements. The conversion $x = 0.35$ is different from the cloud point conversion observed by POM at $x_{cp} = 0.45$ because the phase separation at 30°C is obtained directly without any cooling and results only from a decrease in entropy. In all cases a LC nematic phase is observed but we were not able to know experimentally whether it comes after a liq–liq phase separation or it is directly an isotropic-nematic phase separation.

On one hand, $T_{g\beta} \cong -60$°C remains constant during cure while $T_{g\alpha}$ increases with conversion due to an increase in average molar mass of the copolymer. At $x = 1$, $T_{g\alpha}$ reaches a value of −7°C but, on a second scan, this $T_{g\alpha}$ value increases to 5°C certainly due to some post-cure reactions. This second value remains constant for further scans.

On the other hand, the evolution through out the reaction of $T_{N\text{-}I}$ of the LC-rich phase (DSC measurement) is quite different: $T_{N\text{-}I}$ exhibits a very sharp increase above a conversion $x \approx 0.55$ and then remains constant at a value equal to the $T_{N\text{-}I}$ of the neat LC, 60°C. The jump in $T_{N\text{-}I}$ arrives after the gel point of the epoxy-amine rich phase. Indeed, beyond the gel point, elastic properties appear and the free energy of mixing also depends upon the concentration of elastically active network chains [19] which rises from $x = x_{gel}$ until $x = 1$.

In our system cured at 30°C, phase separation is induced isothermally before the gel point by the increase in average molar mass (PIPS) of the epoxy-amine molecules but we think that beyond the gel point, the elastic term of the free energy of mixing contributes to the phase separation and can be responsible for the sharp increase in $T_{N\text{-}I}$. Another example of the role of elasticity will be given in the next paragraph.

The second isothermal reaction temperature was $T_i = 100$°C, a temperature higher than the $T_{N\text{-}I}$ of the neat LC. We have reported previously [21] that at 100°C gelation of the epoxy-amine matrix occurs at $x_{gel} = 0.61$ and the reactive system remains homogeneous through out the reaction in the range of investigation of the light transmission technique used. (No particles were observed with polariser and analyser parallel to each other). However, it might be possible that a liq – liq phase separation occurred but either the indices of the segregated phases in the isotropic state are too close to one another giving no contrast [13], or the size of the separated phase is not in the range of visible light.

These hypothesis are now considered. First, small angle X-ray scattering (SAXS) was used to detect the appearance of heterogeneities during the reaction at 100°C. No scattering profile was detected which confirms that the mixture is quite homogeneous in the nanometer range (2-50 nm) at 100°C through out the reaction. Secondly, the refractive index of the neat matrix was measured in the course of the polymerization before the gel point. Values of 1.512, 1.520, 1.535 were obtained respectively at conversions $x = 0, 0.30, 0.57$. Besides, the fully crosslinked neat network can be swollen by 31%wt LC at 100°C (Fig. 3). The refractive index of the LC in the isotropic phase can be calculated by $n_i = (n_e + 2n_0)/3 = 1.596$. A first approximation of the refractive index of a homogeneous 31% wt LC swollen network is calculated by an associative law giving $n = 1.554$. Considering that the matrix index was only evaluated up to the gel point but is still increasing after gelation, the refractive index difference between the swollen network and the isotropic LC is small and can prevent an observation by POM of phase separation in the isotropic state.

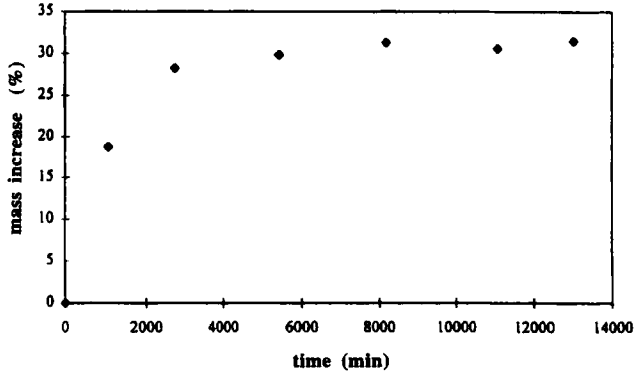

FIGURE 3 Swelling of the fully crosslinked network by the LC (E7) at 100°C.

Thus, at 100°C, the experimental evidence do not show any liq.–liq. phase separation in a 50/50% LC system even though calculations made on the same system predict a liq.–liq. equilibrium at 100°C at a conversion above the gel point [22].

At this stage of the discussion, another fact accounting for the difference between predictions and experiments is that the predictions of demixing curves are based on equilibrium considerations (equality of chemical potentials of each component in both phases) whereas the experiment may not be carried out at equilibrium when the sample has just reached the end of cure at 100°C. To check this latter possibility, we crosslinked a 50/50% mixture in bulk with a free standing surface at 100°C until full conversion. The choice of a bulk sample is made to avoid any effect of confinement of the LC on the phase separation process. Then, we observed the evolution of the sample with time at 100°C ($t=0$ being the end of the cure). As we mentioned previously, no phase separation is observed at 100°C just after the final conversion ($x=1$) is attained and the system appears homogeneous. However, at longer times (several days after sample preparation), the free standing surface gets wet because some LC is slowly expelled out of the gel. $T_{I\text{-}N}$ of the expelled LC is 59°C which means that it is neat LC. To quantify the effect, a deswelling experiment was carried out at 100°C i.e., the surface of the sample is wiped up carefully with tissue paper and the sample is weighed at room temperature as a function of time. The sample is kept at 100°C between each measurement and wiped up before weighing. It was found that, after 15 days, the weight loss was about 4% but the sample surface was still exuding some liquid crystal. This phenomenon is characteristic of macrosyneresis.

K. Dusek has studied the concept of syneresis for the phase separation in network/solvent systems [19]. He introduced two types of syneresis:

i) macrosyneresis or deswelling; which is an equilibrium form of phase separation and where x_{cp} can be predicted. This type of phase separation leads to the formation of continuous liquid and gel phases (the liquid is expelled out of the gel phase).
ii) microsyneresis; which is a non equilibrium form of phase separation in swollen gels. Microsyneresis results in the formation of a dispersed liquid phase in the gel. This kind of phase separation has been predicted and observed experimentally in two cases [19]:

- a swollen network with a constant and low crosslinking density. Microsyneresis is induced upon cooling. Since microsyneresis is a non equilibrium state, the dispersed liquid phase can be slowly expelled out of the gel at long times.
- a swollen network during its formation. Microsyneresis occurs if the solvent concentration exceeds a critical value and if the crosslinking rate is fast enough compared to the macrosyneresis rate. In this case, microsyneresis becomes a stable form of phase separation at full crosslinking and the morphology can be fixed.

Therefore, it is assumed that the bulk epoxy-amine network containing 50% bw LC is in off equilibrium conditions just after reaching full conversion and reaches equilibrium with time (macrosyneresis) at 100°C. However, samples between glass plates do not show this effect during the time scale of study because of the confinement. The role of the glass plates is to confine the mixture and to penalise macrosyneresis due to mechanical constraints.

Although no microphase separation (microsyneresis) was detected in the course of polymerization at 100°C, demixing was clearly detected on cooling different samples depending upon the advancement of the reaction from 100°C to different $T_{I\text{-}N}$. One has to be aware that, in this process, the cooling rate and the quench depth can affect the morphologies and even the equilibrium conditions might not be reached.

Figure 4 gives the evolution with conversion of the transition temperatures as measured by DSC; the evolution of the glass transition temperatures is similar to that of the system cured at 30°C : $T_{g\beta}$ remains constant and $T_{g\alpha}$ increases with conversion. However, the conversion at which two glass transition temperatures are measured for the first time by DSC for the system cured at 100°C and 30°C are different, $x = 0.2$ and 0.35

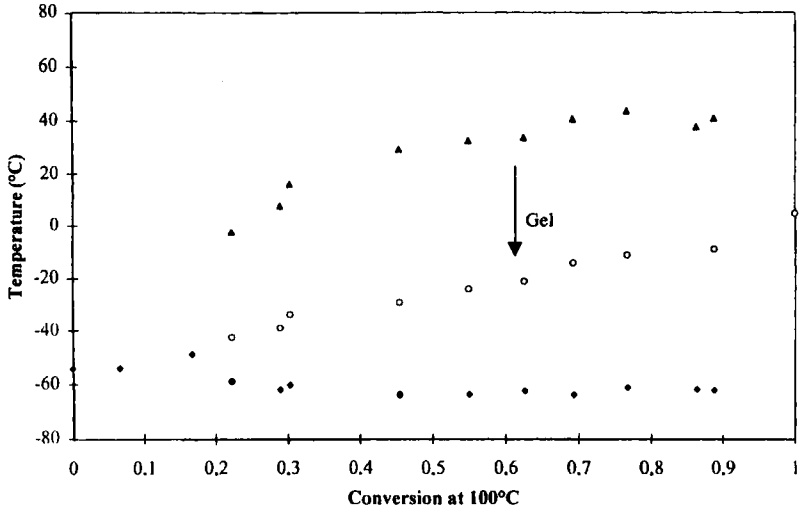

FIGURE 4 Evolution with conversion attained at 100°C of the different transition temperatures for the 50% b/w LC system (thermal conditions: cooling from 100°C to −100°C and then scanning between −100 and 320°C at a rate of 10 K/min).
▲ $T_{N\text{-}I}$ ○ $T_{g\alpha}$ ◆ $T_{g\beta}$.

respectively. The difference may again arise from the fact that the two systems in the DSC are in different non equilibrium states when scanning from −100°C to 320°C. In both systems, $T_{N\text{-}I}$ increases with conversion even after gelation of the epoxy-amine network has been attained ($x_{gel} = 0.61$ if $T_i = 100$°C). The final $T_{N\text{-}I}$ value for the PDLC reacted at 100°C is much lower than the PDLC reacted at 30°C which is that of the neat LC.

Reactive Blends Pre-cured at T_i = 100°C and Post-cured at a Lower Temperature, T_i = 30°C

The reaction rate at 30°C is very slow, so in order to improve the rate of the reaction, the reaction was begun at 100°C, and at different conversions (x_{100}) the samples were cooled to 30°C, and then the reaction was continued at 30°C up to full conversion. Figure 5 gives a scheme of cure cycles and $T_{I\text{-}N}$ values (POM measurements). Here phase separation is detected under POM, during cooling from 100°C, at a cloud point temperature $T_{cp} = T_{I\text{-}N}$ which depends on the pre-cure stage, x_{100}, i.e., the conversion which is reached at 100°C. The cooling rate is much faster than the reaction rate at 30°C [21]; for example, a cooling at a rate of 1 K/min from $x_{100} = 0.45$ implies a cooling time during which the increase in conversion is less than

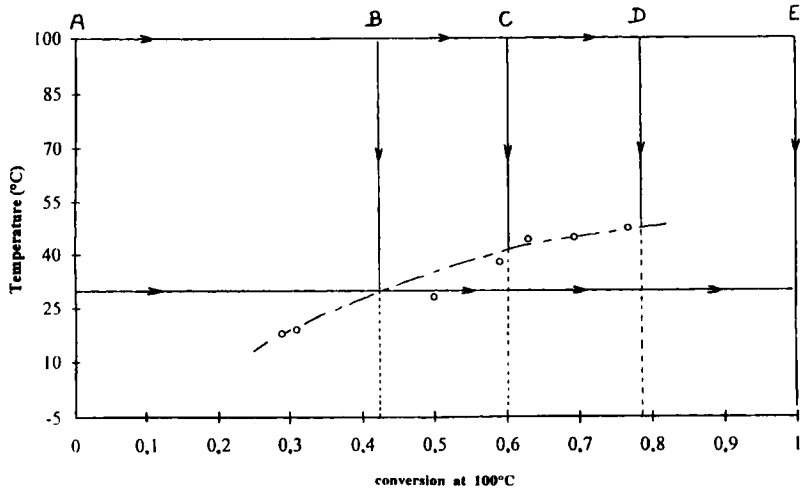

FIGURE 5 Schematic representation of the cure cycles and evolution of cloud point temperatures $T_{I\text{-}N}$ (POM) with conversion attained at 100°C.

1%. Therefore, the cooling is done at constant conversion. At the cloud point, the particles exhibit the same size (birefringent points) whatever the conversion attained at 100°C. Then, the particles grow with conversion at 30°C and the size of the droplets at full conversion is plotted in Figure 1. So now, the samples that we will compare are fully cured but with different pre-cure stage x_{100}.

Figure 5 shows the limits of the cure cycles. Sample A corresponds to $x_{100} = 0$ and sample E to $x_{100} = 1$ i.e., these two samples are cured isothermally at 30 and 100°C respectively up to the maximum conversion. Sample B corresponds to the cloud point $T_{cp} = T_{I\text{-}N} = 30$°C. The particle diameter for this sample at maximum conversion is comparable to the particle diameter of the sample which is cured isothermally at 30°C, $D \approx 25\,\mu m$ (see Figure 1). All samples between A and B are such that their $T_{I\text{-}N}$ are lower than the cure temperature (30°C). Therefore samples between A and B does not phase separate before their $T_{I\text{-}N}$ has reached 30°C which is the intersection of the $T_{I\text{-}N}$-curve and the isotherm line $T = 30$°C (point B). This means that all samples between A and B will separate at the same point B and will have nearly the same diameter at full conversion (Fig. 1). The situation is different for all the samples after B such as those denoted by C, D. $T_{I\text{-}N}$ is now higher than the post cure temperature, thus on cooling from 100°C a nematic phase appears above 30°C.

The main effect of the precuring stage at $T_i = 100$°C between point B and point E is to increase the viscosity of the reaction medium from which the

isotropic-nematic transition occurs when the sample. The increase in viscosity is known to induce a decrease of nucleation and growth rates and of course a decrease in the size of the dispersed particles [24]. It is exactly what is observed in Figure 1 where average diameters of the fully cured samples decrease with increasing x_{100}. Beyond $x_{100} = 0.75$ (point D) and up to $x_{100} = 1$ (point E) no particles are observed under POM between two glass plates : the droplet size is becoming too small to be detected optically.

These two types of experiments [$x_{100} = 0$, $T_i = 30°C$] and [$T_i = 100°C$ up to x_{100} then $T_i = 30°C$ up to $x = 1$] show that the cure cycles have a strong influence on the size of the dispersed nematic phase. Similar observations have been made on such thermal effects on the crystallization and melting of semi-crystalline polymers [25–27]; in both cases the effects are the results of an influence of the viscosity on the nucleation and growth rates of ordered particles.

Phase Compositions After Curing at T_f

For the analysis of phase compositions, the calorimetric data can be worked out in two ways: using T_g and ΔC_p or using $\Delta H_{N\text{-}I}$.

i) Using $\Delta H_{N\text{-}I}$ and ΔC_p related to the β phase, G. W. Smith *et al.* [7] have experimentally determined the "solubility limit of the LC in the matrix" and the fraction of LC contained in the droplets of epoxy based PDLC's containing varying initial amounts of LC. They proposed some relationships which showed a good agreement with their experimental data. These relationships are the following:

$$\frac{\Delta C_p(\beta)^{obs}}{\Delta C_p(LC)} = \frac{\Delta H_{N-I}(\beta)^{obs}}{\Delta H_{N-I}(LC)} = \frac{M_{LC} - A}{1 - A} \tag{1}$$

$$M_{LC}sep = (1/M_{LC})(M_{LC} - A)/(1 - A) \tag{2}$$

(β) refers to the LC-rich phase, (α) refers to the polymer-rich phase
"M" stands for mass fractions, "m" stands for masses, "EA" stands for epoxy-amine
(obs) stands for observed, "sep" for separated
x: reaction conversion
M_{LC}: mass fraction of LC in the initial mixture ($M_{LC} = m_{LC}/(m_{LC} + m_{EA})$)

A : "solubility limit" of the LC in the cured matrix [7] i.e., mass fraction of LC in polymer matrix, $A = M_{LC,\alpha} = m_{LC^\alpha}/m^\alpha$
$\Delta H_{N\text{-}I}$(LC): enthalpy of the N-I transition of neat LC (per unit mass of neat LC)
$\Delta H_{N\text{-}I},(\beta)^{obs}$: enthalpy of the N-I transition in the PDLC (per unit mass of PDLC sample)
$\Delta C_p(\beta)^{obs}$: change in heat capacity of β phase (per unit mass of PDLC sample)
$\Delta C_{p^{LC}}$: change in heat capacity of neat LC (per unit mass of neat LC)
M_{LC}sep: mass fraction of LC in β phase with respect to the mass of LC in the initial mixture ($M_{LC}\text{sep} = m_{LC}\beta/m_{LC}$)

Eqs. (1) and (2) assume that the LC molecules dissolved in the α phase and all the epoxy/amine i-mers do not contribute to $\Delta H_{N\text{-}I}$, $(\beta)^{obs}$. Also, the solubility is considered independent on the initial LC concentration i.e., the polymer can dissolve all the LC up to the solubility limit and the excess LC separates in droplets. In refs [6, 7], the initial LC mass fraction was varied and the PDLC were analysed at full cure. The solubility limit, A, is defined by $m_{LC^\alpha}/(m_{LC^\alpha} + m_p)$ where m_p is the initial monomer mass equal to the polymer mass at full cure. This definition implies that most of the polymer is contained in the α phase. In contrast to refs [6, 7], we consider that A, $\Delta H_{N\text{-}I}$, $(\beta)^{obs}$ and $\Delta C_p(\beta)^{obs}$ are functions of conversion and we have tried to apply Eqs. (1) and (2) to our systems in the course of the reaction. Finally, the $E7$ LC is a four component mixture that can show preferential dissolution in α or β phase depending on conversion while we have asumed unfractionated LC.

First we calculate experimental values of the ratio $(\Delta C_p(\beta)^{obs}/\Delta C_p(\text{LC}))$, then Eq. (1) allows to calculate values of A as defined by Smith *et al.* [7]. Finally, we calculate the mass fraction of LC which has separated, M_{LC}sep, with Eq. (2). Figures 6a, 6b and 6c represent the variation of M_{LC}sep as a function of conversions attained respectively at $T_i = 100°C$ and $T_i = 30°C$ and for the two-step cure. Figure 6 also show calculated fractions of separated LC from another calculation expressed in the next paragraph.

ii) Using the changes in heat capacities (assumed to be independent of temperature) related to the glass transition temperatures of the α phase, we have attempted to determine the mass fractions of the two separated phases. Same type of relationship has been used by Wagener *et al.*, to determine the amounts of segregated soft and hard segments in the case of microphase separation of segmented polyurethanes [28].

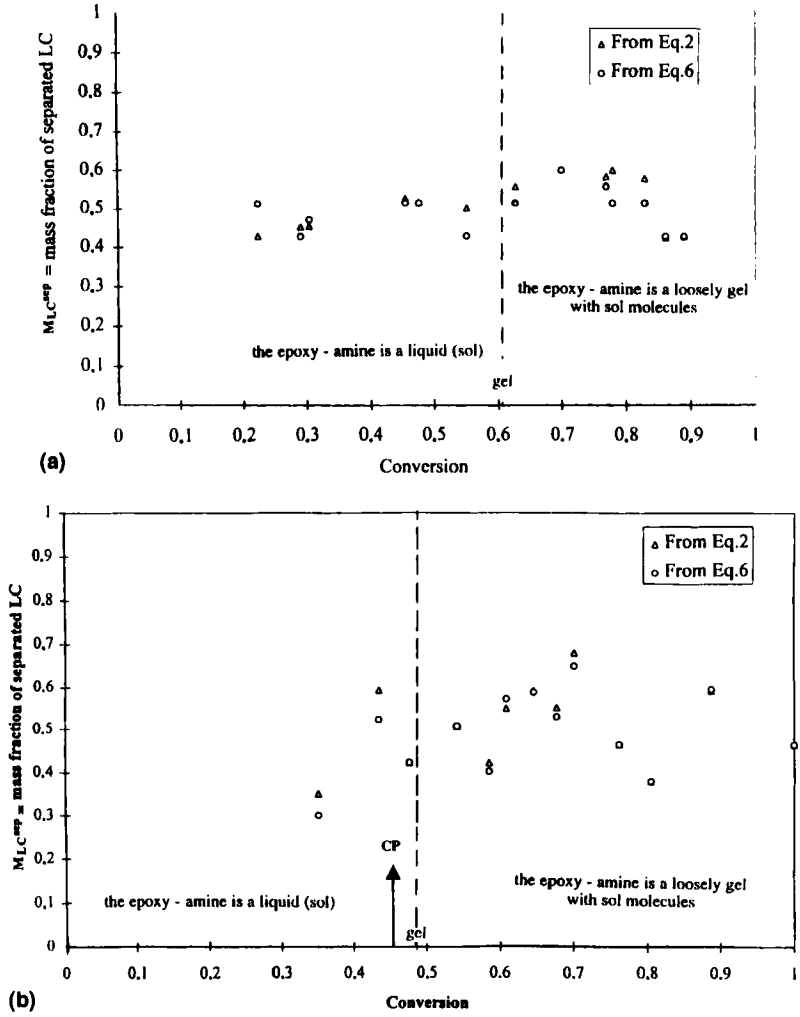

FIGURE 6 Comparison of the mass fraction of LC separated (M_{LC}sep calculated by different equations for the 50% b/w LC system cured:
a) at 100°C △ From Eq. (2) (ref 7) ○ From Eq. (6):
b) at 30°C △ From Eq. (2) (ref 7) ○ From Eq. (6):
c) pre cure at 100°C and post cure at 30°C ■ From Eq. (6).

We can write that the measured ΔC_p of the α phase ($\Delta C_{p_\alpha}^{\text{obs}}$) in the course of the reaction results from a contribution of the epoxy-amine i-mers ($\Delta C_{p^{\text{EA}}}$) and the LC molecules ($\Delta C_{p^{\text{LC}}}$).

$$\frac{\Delta C_{p_\alpha}^{\text{obs}}}{W\alpha} = M_{\text{EA}},\alpha\Delta C_p^{\text{EA}} + (1 - M_{\text{EA}},\alpha)\Delta C_p^{\text{LC}} \tag{3}$$

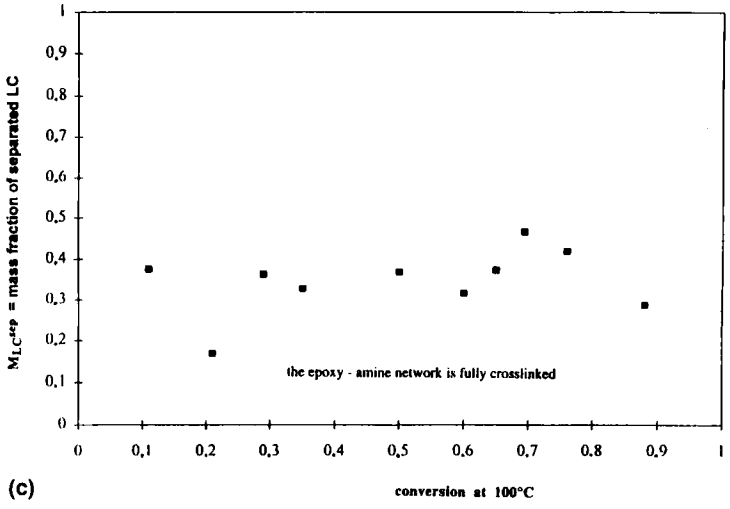

FIGURE 6 (Continued).

where W_α : mass fraction of α-phase, depending on x
$M_{EA,\alpha}$: mass fraction of EA in α-phase also depending on x
We can apply the Fox equation to the T_g values [23]:

$$\frac{1}{T_{g_\alpha}} = \frac{M_{EA,\alpha}}{T_{gEA}} + \frac{1 - M_{EA,\alpha}}{T_{gLC}} \tag{4}$$

T_{gEA} and $\Delta C_{p\,EA}$ depend upon the conversion x [21]. First, $M_{EA,\alpha}$ is calculated from Eq. (4) by measuring $T_{g\alpha}$, T_{gEA} and T_{gLC}. We measure $\Delta C_{p_\alpha}^{obs}$ and as we know $\Delta C_{p\,LC}$ and $\Delta C_{p\,EA}$ as a function of x, we can estimate W_α from Eq. (3). Figures 7a, 7b present the conversion evolution of W_α and W_β. We should always keep in mind that it is only an estimation because there is an uncertainty associated with ΔC_p measurements.

We are also able to calculate the mass fraction of EA in the α-phase (depending upon x) with respect to the mass of EA in the initial mixture:

$$M_{EA}\text{sep} = \frac{M_{EA,\alpha} W_\alpha}{M_{EA}} \tag{5}$$

M_{EA} being the mass fraction of EA introduced in the initial mixture.

The same type of reasoning is done to calculate W_β, $M_{LC,\beta}$ and M_{LC}sep

$$M_{LC}\text{sep}(x) = \frac{M_{LC,\beta} W_\beta}{M_{LC}} = \frac{M_{LC,\beta} W_\beta}{1 - M_{EA}} \tag{6}$$

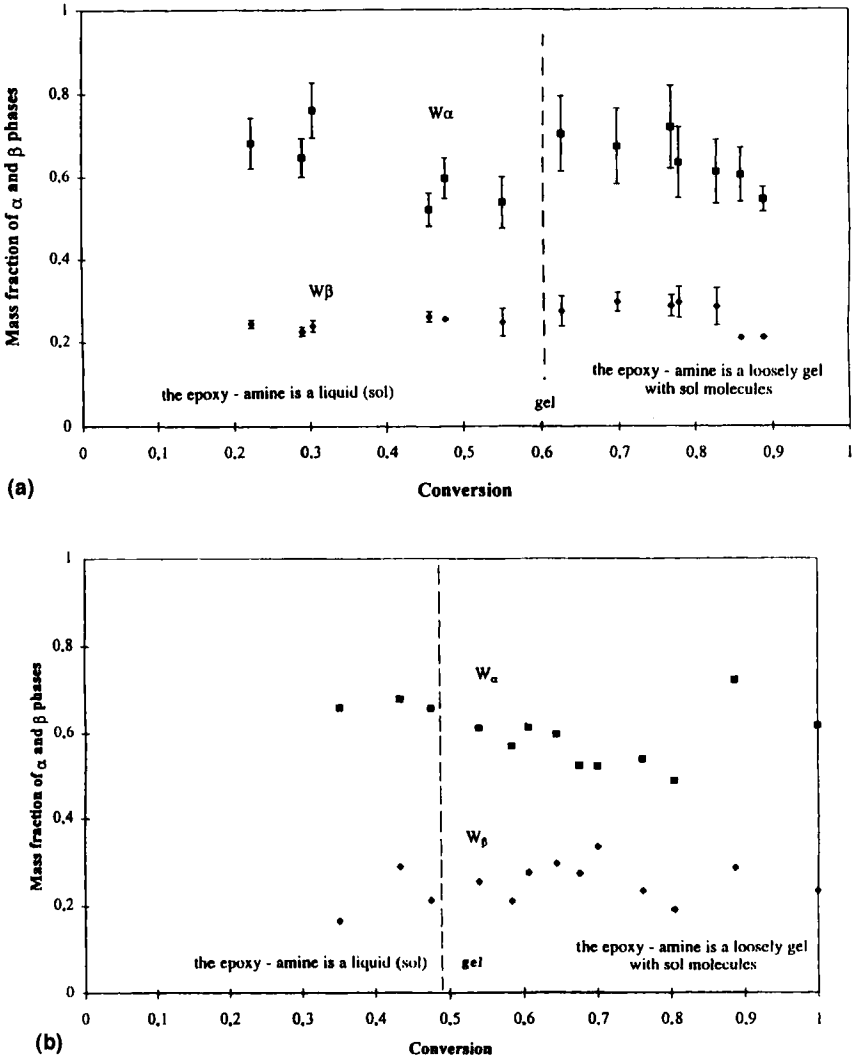

FIGURE 7 Mass fraction dependence of the segregated phases on conversion as calculated by equations (3, 4) for the 50% b/w LC system cured: a) at 100°C b) at 30°C.
■ W_α epoxy-amine--rich phase ◆ W_β LC-rich phase.

W_β: mass fraction of β phase
$M_{LC,\beta}$: mass fraction of LC in β phase
$M_{LC}sep(x)$: mass fraction of LC in β phase, with respect to the mass of LC in the initial mixture, as a function of conversion.

If we compare the two calculation methods, derived from Eqs. (2) or (6), of the fraction of LC in the droplets with respect to the initial mass of LC, one can see a fairly good agreement. Indeed, the calculation of M_{EA}sep from Eq. (5) gives a value close to one which means that all of the polymer is in the α phase. However, this phase contains also an important quantity of LC: only about 50 wt% of the initially introduced LC have phase separated. The solubility limit of the LC in the epoxy-amine network as calculated from Eq. 1 and Figure 6 ranges from 36 to 28.5% (wt% of LC in the gel) when conversion ranges from $x = 0$ to $x = 1$. Also, Figures 6 and 7 reveal that the mass fractions of LC and polymer rich phases (W_β, W_α) and the mass fraction of separated LC (M_{LC}sep) are almost independent on conversion with the thermal conditions used for our calorimetric measurements (cooling to -100°C then scan from -100 to 320°C). The two one-step isothermal cures and the two-step cure provide a similar value of $W_\alpha = 0.60$ to 0.70 (Fig. 7). Thus the cooling process is believed to influence largely phase separation and the calculations based on DSC.

CONCLUSION

Depending upon the cure temperature (T_i), a reactive epoxy-amine/LC (50/50% wt) mixture can undergo either a polymerization induced phase separation (PIPS) or a thermal induced phase separation (TIPS) before gelation. In the observation window investigated and with the techniques used, we have only detected a liquid-nematic phase separation in the form of nematic droplets. In the course of the polycondensation, if T_i is above the N-I transition of the neat LC (in our case $T_i = 100$°C), TIPS is effective only when the partially reacted homogeneous mixture is cooled down from the reaction temperature. On the other hand, if T_i is far below the N-I transition, PIPS occurs isothermally (in our case at $T_i = 30$°C) at a certain conversion x_{CP}.

The glass and the N-I transition temperatures of the blends were measured in the course of the polycondensation. Phase separation is characterized by two T_g's and a $T_{N\text{-}I}$. These calorimetrically determined T_g values were used to calculate the mass fraction of the LC-rich phase and the mass fraction of the separated LC which were found to be nearly conversion independent because of the quench used for the calorimetric measure.

Gelation of the epoxy-amine copolymer does not equally affect the two separation processes (TIPS and PIPS) as far as $T_{N\text{-}I}$ is concerned: $T_{N\text{-}I}$ is almost not sensitive to gelation in the TIPS whereas $T_{N\text{-}I}$ markedly increases near the gel point in the PIPS.

The morphologies were studied during polymerization. When the PDLC results from TIPS, the final morphology depends strongly on the stages of the thermal process (i.e., conversion extent in the homogeneous state followed by conversion extent in the heterogeneous state). In the PIPS isothermal process, morphology is formed isothermally before gelation and the average droplet size rises with conversion. A nucleation-growth-like mechanism is suggested to account for the formation of LC droplets whatever the cure cycles used. Nematic particles in the range of 20–30 μm were formed but the size can be lowered down to micron particles using appropriate cure cycles (e.g., high temperature cure followed by low temperature cure).

Theoretical analysis of the phase separation will be presented to account for these experimental results, especially to investigate the conditions for liquid–liquid phase separation and to check the possibility of having a homogeneous swollen network at 100°C with 50% LC. Simulation of conversion-concentration and temperature-concentration phase diagrams are calculated [22].

Acknowledgement

Dr. Laurent David is greatly acknowledged for performing and discussing SAXS measurements. Mr. J. Maugey is acknowledged for refractive index measurement.

References

[1] H. S. Kitzerow, *Liquid crystals*, **16**, 1 (1994).
[2] J. L. West, *Mol. Cryst. Liq. Cryst.*, **157**, 427 (1988).
[3] R. J. J. Willliams, B. A. Rozenberg and J. P. Pascault, accepted in Adv. in *polym. Sci.*, **128** (1997).
[4] G. W. Smith and N. A. Vaz, *Liquid Crystals*, **3**, 543 (1988).
[5] G. W. Smith, *Mol. Cryst. Liq. Cryst.*, **213**, 11 (1992).
[6] G. W. Smith, *Mol. Cryst. Liq. Cryst.*, **225**, 113 (1993).
[7] G. W. Smith, *Mol. Cryst. Liq. Cryst.*, **237**, 243 (1993).
[8] J. Y. Kim and P. Palffy Muhoray, *Mol. Cryst. Liq. Cryst.*, **203**, 93 (1991).
[9] J. Y. Kim, C. H. Cho, P. Palffy Muhoray, M. Mustafa and T. Kyu, *Phys. Rev. Lett.*, **71**, 2232 (1993).
[10] T. Kyu, M. Mustafa, J. Yang, J. Y. Kim and P. Palffy Muhoray, *Polmer solutions, blends and interfaces*, Elsevier Science Publishers, 245 1992.
[11] J. Lin and P. L. Taylor, *Mol. Cryst. Liq. Cryst.*, **237**, 25 (1993).
[12] A. Golemme, G. Arabia and G. Chidichimo, *Mol. Cryst. Liq. Cryst.*, **243**, 185 (1994).
[13] W. Ahn, C. Y. Kim, H. Kim and S. C. Kim, *Macromolecules*, **25**, 5002 (1992).
[14] A. Matsuyama and T. Kato, *J. Chem. Phys.*, **105**, 1654 (1996).
[15] T. Kyu, I. Ilues and M. Mustafa, *Journal de physique iv*, Colloque C8, supplément au Journal de Physique I, **3**, 37 (1993).

[16] C. Shen and T. Kyu, *J. Chem. Phys.*, **102** (1995).
[17] W. K. Kim and T. Kyu, *Mol. Cryst. Liq. Cryst.*, **250**, 131 (1993).
[18] H. W. Chin, Z. L. Zhou, T. Kyu, L. G. Cada and L. C. Chien, *Macromolecules*, **29**, 1051 (1996).
[19] K. Dusek, Polymer networks: structure and mechanical properties, In *Proceedings of the ACS Symposium on* "Highly Crosslinked Polymer Networks Chicago", sept 14 – 15 (1970).
[20] R. Moerkerke, R. Koningdveld, H. Berghmans, K. Dusek and K. Solc, *Macromolecules*, **28**, 1103 (1995).
[21] H. Masood Siddiqi, M. Dumon, J. P. Eloundou and J. P. Pascault, *Polymer*, **21**, 4795, (1996).
[22] J. Borrajo, C. Riccardi, R. J. J. Williams, H. M. Siddiqi, M. Dumon and J. P. Pascault, accepted in *Polymer*.
[23] T. G. Fox, *Bull. Am. Phys. Soc.*, **2**(2), 123 (1956).
[24] S. Montarnal, *Ph.D thesis*, INSA de Lyon, p-151 1987.
[25] K. Mezghani and paul J. Phillips, *Physical properties of polymers handbook*, American Institute of Physics, 417 (1996).
[26] P. J. Barham, *Material Science and Technology, Vol 12, Structure and properties of polymers*, VCH Weinheim, 153 (1993).
[27] A. Keller, *Macromol. Symp.*, **98**, 1 (1995).
[28] K. B. Wagener and J. C. Matayabas Jr, *Macromolecules*, **24**, 618 (1991).